J. Phys. Chem. A 2004, 108, 4405−4411

Ultraviolet Spectroscopy of Large Water Clusters: Model and Calculations for $(H_2O)_n$, for $n = 8, 11, 20, 40$, and 50

Y. Miller,[†] E. Fredj,[‡] J. N. Harvey,[§] and R. B. Gerber*,[†,#]

Department of Physical Chemistry and The Fritz Haber Research Center, The Hebrew University, Jerusalem 91904, Israel, Computer Science Department, Jerusalem College of Technology—Machon Lev, Jerusalem 91160, Israel, School of Chemistry, University of Bristol, Bristol BS8 1TS, England, and Department of Chemistry, University of California, Irvine, California 92697-2025

Received: May 30, 2003; In Final Form: January 27, 2004

The UV absorption spectra of neat water clusters $(H_2O)_n$ of sizes in the range of $n = 8-50$ are computed. The simple model used for the excited states includes the dependence of the excitonic interactions on both the intermolecular and intramolecular coordinates. For a cluster $(H_2O)_n$, n excitonic potential energy surfaces are computed for geometries in the Franck−Condon region. The Coker−Watts potential is used to describe the interactions in the electronic ground state, and molecular dynamics simulations are performed to sample geometries for the classical Franck−Condon calculations. There are numerous crossings of different excitonic potential surfaces for $(H_2O)_n$ in the range of the geometries sampled. The main findings are (i) the main absorption peak of $(H_2O)_n$ shifts to the blue and increases in width as the cluster size n is increased; (ii) the widths of the absorption bands increase with temperature, e.g., for $(H_2O)_{20}$, the width is 1.2 eV at 80 K and 1.6 eV at 220 K; (iii) several well-resolved peaks within the absorption band are found for some of the systems at certain temperatures, and in such cases, each of the peaks generally results from absorption into different excitonic states; (iv) although the absorption peaks are strongly shifted to the blue, with respect to the (H_2O) monomer, for some cluster sizes, a weak absorption tail to the red side is also observed as the temperature increases.

I. Introduction

Water clusters of different size ranges have been extensively studied recently, both experimentally and theoretically.[1] Much progress has been made on the characterization and understanding of many properties of these systems. This is the case for the vibrational spectroscopy of these clusters, which has blossomed into a broad area of research, with the introduction of novel experimental techniques and the development of improved theoretical models. It is especially true for relatively small clusters, with rigorous calculations and simulations.[2−13] The situation is quite different for the electronic spectroscopy of neat water clusters. Relatively little seems to be known on this topic, although it is of potential importance for the understanding of a range of phenomena. For example, electronic spectroscopy is essential for the study of photochemical processes, and water clusters offer a very interesting framework for the exploration of photochemistry in hydrogen-bonded networks. The electronic spectroscopy of finite water clusters is very useful for understanding the electronic properties of liquid water in bulk, and those of ices. The excited electronic states of the water molecule, and the related photodissociation dynamics in the gas phase, have been studied in detail. The UV absorption cross sections of the three lowest bands ($\tilde{A}^1B_1$, $\tilde{B}^1A_1$, and $\tilde{C}^1B_1$, respectively) were measured[14] and ab initio calculations of the excited electronic states and the transition moments were reported.[15]

There is a wealth of experimental data on vibrational and rotational state distributions on the electronic states of the photofragments and on vibrational and rotational product state distributions.[16−19] Good potential energy surfaces are available from ab initio calculations.[20,21] Finally, extensive calculations on the photodissociation dynamics have been reported.[9,22] Such detailed data are not available for water clusters. Ab initio calculations on the lowest excited singlet state of small water clusters have been performed by van Hemert and van der Avoird,[23] Sosa et al.,[24] and Sobolewski and Domcke.[25] Useful hints on the UV spectroscopy of water clusters can be inferred from experimental data on spectroscopy and photodissociation of liquid water and of ice in bulk.[26−28] Model calculations of electronic excitation spectra of water in bulk are also available.[29−31] The present study continues and expands on a previous theoretical investigation by Harvey, Jung, and Gerber.[32] In that paper, the UV absorption spectra of small water clusters $(H_2O)_n$, where $n = 2-6$, were calculated from a theoretical model of excited electronic states. The calculations were conducted for water clusters initially at 0 K, i.e., in the vibrational ground state. In the present paper, we use the same simple model for the excited-state potential to explore the UV absorption spectrum of water clusters $(H_2O)_n$ of various sizes (up to $n = 50$). In addition, we study the temperature dependence of the absorption bands. In some of the calculations, the clusters are in a “solid-like” state, whereas in other calculations, their state is essentially in the liquid regime. The objective of these calculations is to serve as a guide for future experiments.

The structure of the article is as follows. The theoretical model used in the calculations is presented in Section II. The results of the simulations are described and discussed in Section III. Concluding remarks are presented in Section IV.

---

* Author to whom correspondence should be addressed. E-mail address: Benny@batata.fh.huji.ac.il.

[†] The Hebrew University.

[‡] Jerusalem College of Technology—Machon Lev.

[§] University of Bristol.

[#] University of California, Irvine.

10.1021/jp030678b CCC: $27.50

II. Model and Methods

To determine trends in the dependence of the spectroscopy on cluster size, we performed calculations for the cluster sizes $n = 8$, 11, 20, 40, and 50. The UV spectra of smaller water clusters ($n = 2-6$) were studied theoretically by Harvey et al.[32] That study was limited to clusters initially in their vibrational ground state. In the present paper, we investigate the temperature dependence of the electronic absorption spectroscopy for clusters in the temperature range from $T = 50$ K to $T = 300$ K. This range covers both solid-like and liquid-like states of the clusters.

A. Simulations of the Initial State. Calculation of the Franck–Condon factors requires sampling of the configurations of the system at a given temperature. We assume that, for the temperatures considered here ($T \geq 50$ K), classical dynamics can be used for the purpose of sampling configurations. Obviously, the temperatures considered are very low, compared with the zero-point energies of the stiff intramolecular vibrations. However, the distribution of cluster configurations is mostly determined by the soft intermolecular motions of the water molecules, and for these low-frequency modes, classical dynamics should be a reasonable approximation at and above 50 K. However, the intramolecular vibrations of the monomers were included in the modeling. We used the Coker–Watts potentials[33] for the intramolecular force field and for interactions between water molecules in the electronic ground state. The Coker–Watts model is not the most-accurate potential currently available for the interaction between vibrationally flexible water molecules; for example, it does not include three-body and higher-order effects. However, the objectives of this study are only semiquantitative, and we estimate that, for this purpose, the accuracy of the Coker–Watts model is sufficient. The Coker–Watts modes were adopted here for their computational convenience. To sample configurations for a cluster at a given temperature, molecular dynamics (MD) simulations were performed. The trajectories were computed using the standard Verlet algorithm and propagated in time to equilibration.[34] The standard MD tests have shown that equilibrium was attained within time scales on the order of 20 ps. (The equilibration time differs for each system.) The propagation of the trajectories was pursued beyond equilibration, and configurations were sampled at random times. The set of these configurations represents a sampling of the equilibrium state of the cluster, and photoexcitation is assumed to occur from this initial state. Each simulation involved the calculation of a single, sufficiently long trajectory for a fixed, conserved total energy. The temperature of such a fixed-energy system obviously fluctuates in time; however, the fluctuations were computed and determined to be very small ($\Delta T \lesssim 1$ K, typically). Thus, the temperature was practically well-defined in the simulations.

There are large-amplitude motions in the clusters at the temperatures studied. Nevertheless, the minimum-energy structure is often useful for interpretation and analysis. Thus, a search for the most-stable structure was conducted for each cluster. In several cases, other low-energy isomers were computed, because knowledge of these structures can also be useful in the interpretation of the spectra. The calculation of the structures was performed by the simulated annealing method. There is no certainty in these calculations that, indeed, the global minimum structure would be determined. Given the extensive searches that we pursued, we assume that the lowest-energy isomer was determined in most cases. Except for the lowest temperatures used, several local minimum structures are sampled by the trajectories; however, these structures are not necessarily very different geometrically. The low-temperature simulations seem to be confined to the vicinity of the global minimum structure.

B. Modeling of the Excited Electronic States. The excitation modeled in the present study corresponds to the $\tilde{A}^1B_1$ band in the case of the monomer, which is the lowest excitation band. Consider the cluster $(H_2O)_n$ for a first configuration of the atoms. If interactions between the water molecules are ignored, there are n nearly degenerate excited energies in the band for that configuration, each corresponding to an excitation of a different water molecule in the cluster. The excitation energies of different water molecules can differ, if their internal geometries are slightly different, representing different vibrational displacements from equilibrium. The n excited states are exactly degenerate for configurations where all molecules in the cluster have exactly the same vibrational displacements. When the effects of interactions between the water molecules are incorporated, including interaction between the excited monomer and the other molecules, the result will be the formation of n excitonic states from the n localized excited states of the different H_2O molecules. When treating the excitonic states, we followed the model of Harvey et al.[32] previously used for $(H_2O)_n$, for $n = 2-6$. We constructed the matrix Hamiltonian in the representation of the basis of the uncoupled water molecules. The ith basis function can be written as

$$\Phi_i^{(0)} = \Phi_i^{(\mathrm{ex})}(r_i,R_i)\prod_{j\neq i}\phi_j^{(g)}(r_j,R_j) \tag{1}$$

where r_i denotes the electronic coordinates of the ith water molecule, and R_i is the nuclear configuration of that same molecule. $\Phi_i^{(\mathrm{ex})}$ is the excited state of the ith water molecule, and $\Phi_j^{(g)}$ denotes the ground electronic state of molecule j. Specifically, the excited state of $\Phi_i^{(\mathrm{ex})}(r_i,R_i)$ is the $\tilde{A}^1B_1$ state of water. Studies of the water monomer indicated that the $^1B_1$ state is obtained by promoting an electron from the lone-pair $1b_1$ orbital of the ground state into the part-Rydberg, part-antibonding $4a_l$ orbital.[15,20] The diagonal elements H_{ii} of the Hamiltonian model in the representation of the basis described in eq 1 are given by[32]

$$H_{ii} = V^{i*} + \sum_j V^{i*,j} + \sum_{j\neq i} V^j + \sum_{j<k\neq i} V^{j,k} \tag{2}$$

In this equation, $i*$ refers to the ith water molecule in the excited state, j and k refer to water molecules in the ground state. The last two terms represent the intramolecular and intermolecular contributions to the potential from the ground-state molecules, for which we used the Coker–Watts model.[34] V^{i*} is the excited-state potential surface of the ith monomer, which describes the intramolecular potential of the excited water molecule. We used the analytic representation of Engel et al.,[35] which was obtained by fitting the ab initio points of Palma and Staemmler.[38] The second term in eq 2 represents the interaction between the excited molecule i and the other ground-state molecules. It is assumed that this interaction is a sum of pairwise interactions between i and each of the ground-state molecules. The interaction potential $V^{i*,j}$ is represented in the form

$$V^{i*,j} = V_{\mathrm{O}_{i*},\mathrm{O}_j} + V_{\mathrm{O}_{i*},\mathrm{H}_j} + V_{\mathrm{H}_{i*},\mathrm{O}_j} + V_{\mathrm{H}_{i*},\mathrm{H}_j} + \sum_{\alpha,\beta}\frac{q_{i*\alpha}q_{j\beta}}{R_{i*\alpha,j\beta}} \tag{3}$$

The last term in eq 3 represents the Coulomb interactions between partial charges on the excited molecule $i*$ and the ground-state molecule j. α labels the partial charge sites on $i*$, and β is an index of the partial charge sites on the ground-state molecule. The partial charges for the ground-state molecule were taken from Coker and Watts.[33] The partial charges on i^* were determined, to reproduce the dipole moment of excited H_2O (from ab initio calculations). This dipole moment is in the opposite direction to that of the ground state. The dipole moment of the excited water molecule $(H_2O)^*$ is reproduced by placing negative charges of -0.225 au on the H atoms, and a positive charge of 0.45 au at the center of mass. The atom−atom potentials $V_{O_i^*,O_j}$, $V_{O_i^*,H_j}$, and $V_{H_i^*,H_j}$ were modeled as repulsive exponentials, whereas $V_{H_i^*,O_j}$ was assumed to be a Morse function. The parameters of all these pairwise interactions were determined by fitting $V^{i^*,j}$ to ab initio calculations of that interaction in the $(H_2O)^*-H_2O$ dimer.[32] Approximately 200 ab initio interaction points were computed using the MCQDPT2 method. The excited-state water molecule is known to be highly polarizable.[15,36] This is not explicitly treated by our model, and we assume that this effect is implicitly incorporated by the parameter values, through their determination by fitting ab initio calculations. Note that, in the limit of strong interactions between water molecules, the pairwise treatment of the diagonal portion of the excited-state potential may break down. For example, the diffuse, Rydberg-like electron of the $\tilde{A}^1B_1$ state of the monomer may be polarized away from the excited molecule, leaving an H_2O^+ core and a delocalized electron cloud. Equally, the Rydberg-like orbital could be localized to yield a valence-state excited water molecule, in which the excited electron occupies a purely antibonding orbital. This can be expressed in different terms, with adjacent ground-state water molecules inducing mixing of the various excited states of the water molecule, such that even the lowest excited manifold of water clusters is not composed solely of combinations of $\tilde{A}^1B_1$-like states, as assumed in our model. We note that some test MCQDPT2 calculations have been performed on the trimer, which give fair agreement with the predictions of the simple model, despite the fact that the latter was parametrized only for dimer systems. This suggests that the aforementioned problems may not be too severe; however, the present work must be considered to be preliminary, and further tests of the performance of the potential are needed. Nevertheless, the qualitative results of our work should give useful insight into the nature of the excited states of water clusters.

The off-diagonal elements H_{ij} of the model Hamiltonian are assumed to be dominated by the interaction between the transition dipole moments of the monomers i and j. The dipole−dipole interaction is a term in the multipolar expansion of the potential between an electronic excited species and a ground-state species; however, when the transition dipole is large, this term often dominates. An analytic expression is used[38] in the model for the transition dipole moment, the direction of which is orthogonal to the plane of the water molecule. The origin of the transition moment vector is located at the molecular center of mass. We note that, in the geometries used to determine the potential parameters in eq 2, the dipole−dipole interaction, by symmetry, is zero.[32] Ab initio calculations at other geometries of $(H_2O)^*-H_2O$ yield excitonic splittings,[32] which our model attributes to the dipole−dipole interaction. The predictions of the dipole−dipole model were tested directly against ab initio calculations in the case of the $(H_2O)^*-H_2O$ dimer and are in good agreement, at least for the range of distances that are relevant here.

The diagonalization of the model Hamiltonian for a given nuclear configuration yields n energy levels. These constitute the excitonic $^1B_1$, band of $(H_2O)_n$ for that given configuration. The energies obviously are dependent on the nuclear configuration. Note that the model explicitly includes the dependence on both the intramolecular and intermolecular geometries. The wave functions determined in the diagonalization process, which are eigenfunctions of the model Hamiltonian, are the excitonic states. Analysis of these eigenfunctions can reveal the extent to which these excitonic states are localized on the monomers, or perhaps delocalized. Recall that the bands that correspond to absorption continua of the $\tilde{B}^1A_1$ and $\tilde{C}^1B_1$ states of the monomer are completely neglected in this model. As we shall see later, the results predict strong blue shifts of the $\tilde{A}^1B_1$ band, compared with the position in the monomer. It is expected that inclusion of the higher states in the model could limit the magnitude of the computed blue shifts. Unfortunately, such an extension of the model is complicated and remains a challenge for the future.

The model Hamiltonian can be expected to be valid only in the Franck−Condon region for very short time durations after photoexcitation. Photoabsorption will, after some time, lead to photodissociation of a monomer in the cluster:

$$H_2O(\tilde{X}^1A_1) + \hbar\omega \rightarrow H_2O(\tilde{A}^1B_1) \rightarrow H(^2S) + OH(X^2\Pi)$$

The H atom, which is released with high kinetic energy, can induce further chemical processes. The model Hamiltonian cannot describe the photodissociation process, and it is not applicable beyond the photoexcitation stage.

C. Calculation of the Absorption Spectra. The calculations presented here of the absorption intensities, as a function of excitation energy, use a simple classical Franck−Condon approximation. For each nuclear configuration R, which is sampled from the MD simulations at equilibrium, a vertical promotion into the excited-state potential surfaces is assumed to occur upon photodissociation. The excited-state energies for that configuration are computed by diagonalization of the model Hamiltonian at the configuration R. For a cluster $(H_2O)_n$, there are up to n distinct excitonic levels. In obtaining the absorption intensities, the assumption was made that the transition moments into the various excitonic states are independent of R. This, in fact, suggests that the distribution of cluster geometries is far more sensitive to nuclear positions than the transition moments. We note that, in the study by Harvey et al.[32] on the smaller clusters, the dependence of the transition moments on nuclear positions was treated by an approximate model. Thus, the present treatment is cruder; however, for larger systems, this seems more justifiable. Classically, the probability of photoabsorption at a range ΔR around R in configuration space is proportional to the time the (equilibrated) trajectory spends in that region of configuration space, and, therefore, is proportional to the number of configurations sampled in that region. Thus, a histogram is constructed such that $N(E)\Delta E$ is the number of sampled points with corresponding excitation energy between $E - \Delta E/2$ and $E + \Delta E/2$. The plot of $N(E)$ versus E (for a chosen “energy bin” of ΔE) is given in the same relative units as the graph of the absorption intensity $I(E)$ against the excitation energy. This only provides a coarse absorption lineshape. Not only are quantum effects such as interference completely absent, but also features of a classical nature may be lost, because of insufficient density of sample configurations. Nevertheless, this suffices for a semiquantitative description of the spectra. It was observed in the calculations that the excitation energies are most sensitive to a specific geometric aspect of the configuration. This is the orientation of the excited molecule $(H_2O)^*$, with regard to the nearest ground-state H_2O bound to it as an acceptor of the hydrogen bond. Denoting the OH dipole axis of $(H_2O)^*$

(the H atom is the donor in the hydrogen bond) by μ_A, and denoting the OH dipole direction in the nearest-neighbor H_2O by μ_B, one can define an "orientation" angle θ by

$$\cos\theta = \frac{\mu_A \cdot \mu_B}{|\mu_A||\mu_B|} \tag{4}$$

It was found that this angle is the configurational parameter that most strongly affects (at least on average) the excitation energies. In our analysis of the spectra, we emphasize the role of the configurations—and, in particular, the role of the angle θ—in determining the excitonic levels. This provides very helpful insights into the computed spectra.

III. Results and Discussion

It is useful to mention at the outset the main results of ref 32 on the electronic spectroscopy of the small clusters $(H_2O)_n$, for $n = 2-6$. These calculations were made for clusters initially in their ground vibrational state. It was found that (i) the spectra all show a single major peak; (b) the spectra are shifted to the blue, with respect to the water molecule; (iii) the shift to the blue increases with cluster size, and (iv) among the smaller clusters, only the dimer also shows (in addition to the strong blue shift) a weak absorption tail to the red of the water molecule. This prediction is supported by later experiments by Imura and co-workers.[39] We note that the absorption lineshapes shown in ref 32 involve a technical error that is, however, quantitatively small and should not affect the present discussion.

A. Equilibrium Structures. Knowledge of the equilibrium structure of the clusters seems to be helpful for the interpretation of some results. The structures shown in Figure 1, which were obtained by simulated annealing calculations, are likely to be the global minimum structures for the potentials used. (As noted in Section II, we assume this is the case, in view of the extensive search made.) Recall that, at the lowest temperature considered, $T = 50$ K, all the clusters are essentially in a "solid-like" state, and the excursions from the equilibrium configuration are moderate. At the highest temperature studied, $T = 300$ K, all the clusters, including the largest ones, are in a liquid-like state and configurations from the global minimum are visited in the course of the motions. Several local minima are visited by the MD trajectories at the higher temperature; however, the system spends more time in the vicinity of the global minimum than in that of any of the other local minima.

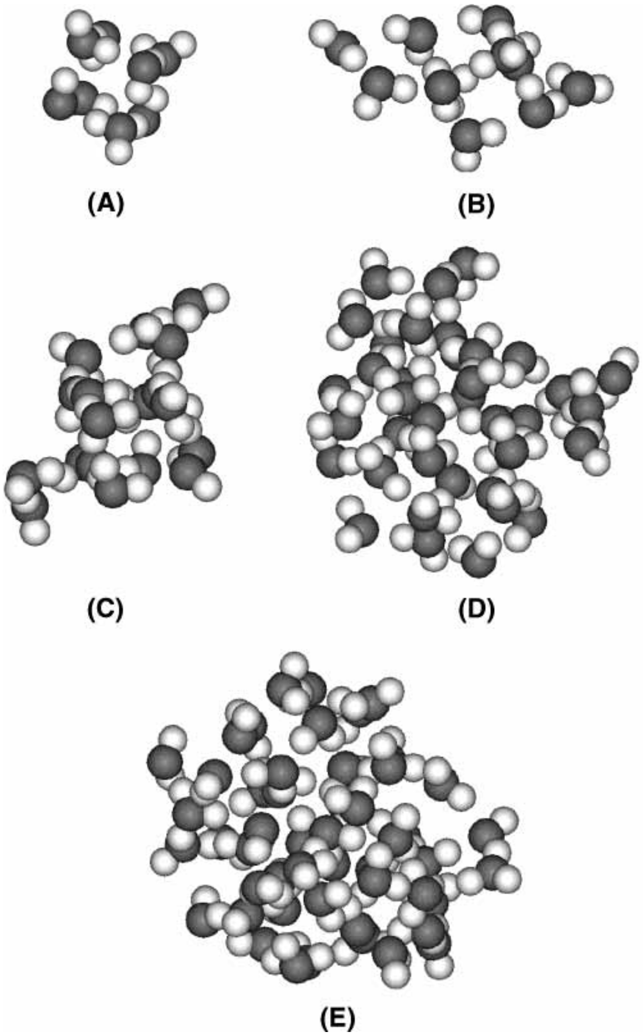

Figure 1. Computed equilibrium structures of (A) $(H_2O)_8$, (B) $(H_2O)_{11}$, (C) $(H_2O)_{20}$, (D) $(H_2O)_{40}$, and (E) $(H_2O)_{50}$.

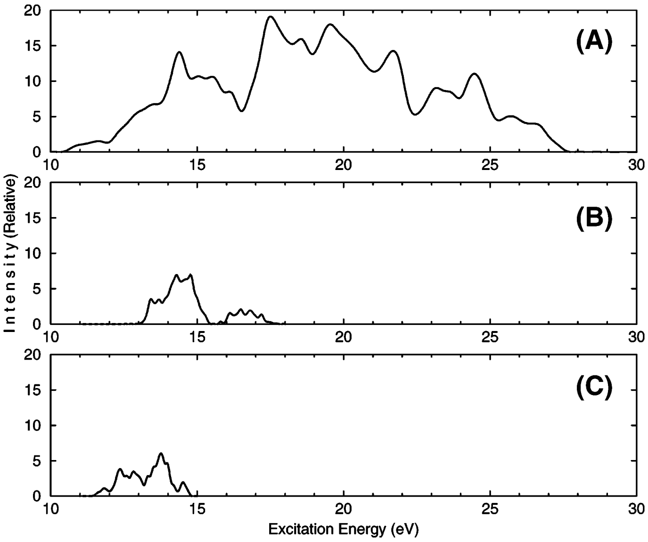

Figure 2. Electronic absorption spectra of (A) $(H_2O)_{50}$, (B) $(H_2O)_{11}$, and (C) $(H_2O)_8$, each at $T = 250$ K. Intensities are given in relative units, and the excitation energy is given in electron volts.

B. Effects of Cluster Size on the Spectroscopy. Figure 2 shows the electronic absorption spectra of $(H_2O)_8$, $(H_2O)_{11}$, and $(H_2O)_{50}$ at $T = 250$ K. At this temperature, the clusters are in a liquid-like state, with the monomers carrying out large excursions from the global minimum structure. All three spectra are strongly shifted to the blue, compared to that of an isolated water molecule. Furthermore, the shift increases greatly with increasing cluster size. The maximum of the absorption spectrum of $(H_2O)_{11}$ is ~1.3 eV to the blue of the maximum for $(H_2O)_8$; the maximum of the absorption profile of $(H_2O)_{50}$ is shifted by 2.4 eV from the maximum peak position for $(H_2O)_{11}$. The shift to the blue with increasing cluster size of the high-energy tails of the absorption bonds is even more dramatic. All this is consistent with the findings for the small $(H_2O)_n$ clusters[32] and has the same interpretation. The excitation process promotes a lone-pair electron into an orbital of partial-Rydberg character. This electron is repelled by the electron densities around the O atoms of neighboring water molecules, which increases the excitation energy. This "confining box" effect for the promoted electron is larger for more-compact clusters, with more neighboring O atoms available to contribute to the repulsion. However, as mentioned in the Model and Methods section, the diagonal component of the interaction potential in the excited

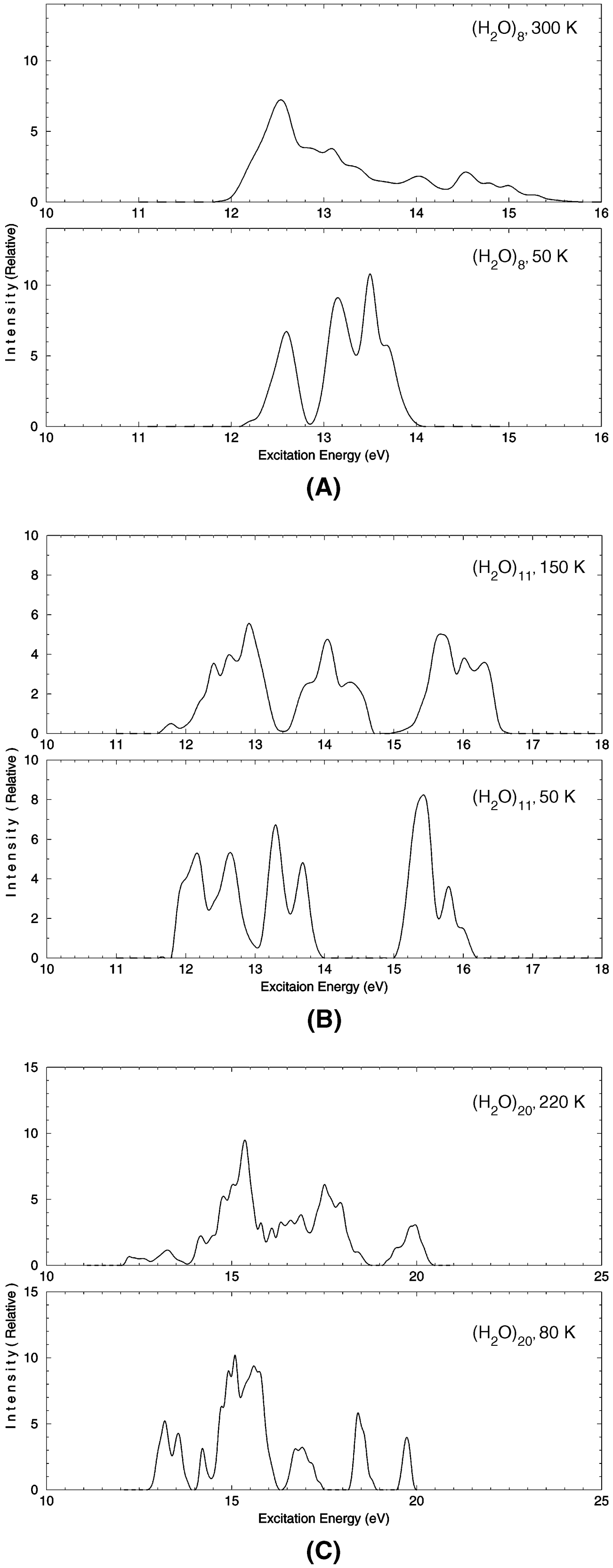

Figure 3. Electronic absorption spectra of (A) $(H_2O)_8$ (at $T = 300$ and 50 K), (B) $(H_2O)_{11}$ (at $T = 150$ and 50 K), and (C) $(H_2O)_{20}$ (at $T = 220$ and 80 K).

states may not reproduce the confining effect accurately, in case the pairwise additivity assumption breaks down. In the presence of more than one neighboring ground-state water molecule, the electronic structure of the excited molecule may be considerably different from that in the dimer, and lower (or higher) energies may be obtained from the excitonic states. The present results suggest that our simple model may indeed exaggerate the confining box effect for larger clusters.

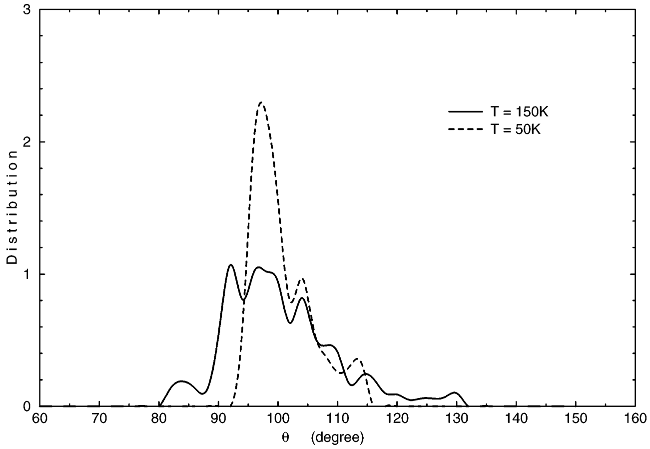

Figure 4. Distribution of torsion angle θ for $(H_2O)_8$ (—) at $T = 150$ K and (− − −) at $T = 50$ K. θ is the angle between an OH axis of the excited water molecule and an OH axis of a neighboring water molecule in the ground state.

Another contributing factor is the increasing number of excitonic levels with n. The width of the spectrum is expected to increase with additional excitonic states. In part, the absorption bands into individual excitonic components overlap; however, at least in several cases, the additional excitonic levels absorb to the blue of the previous ones. Recall that our calculations model only absorption into the band corresponding to $\tilde{A}^1B_1$, in the case of the monomer. For the real systems, other excited bands, such as $\tilde{B}^1A_1$ and $\tilde{C}^1B_1$, are certainly expected to contribute at sufficiently high excitation energy. As noted in the Model and Methods section, inclusion of the higher-energy states is likely to limit the blue-shift effect on $\tilde{A}^1B_1$. Thus, it is possible that the model yields exaggerated blue shifts. This is an important point for future experiments to examine.

C. Effect of Temperature on the Width of the Spectra. Figure 3A compares the absorption spectrum of $(H_2O)_8$ at $T = 300$ K (top) with that at $T = 50$ K (bottom); Figure 3B compares the UV spectrum of $(H_2O)_{11}$ at $T = 150$ K (top) with that at $T = 50$ K (bottom), and Figure 3C shows the spectrum of $(H_2O)_{20}$ at T = 220 K (top) and 80 K (bottom). In all these cases, the total width of the spectrum increases as the temperature increases. The cause for this effect is straightforward. As the temperature increases, the set of configurations accessible to the system in the ground-state becomes larger, and the Franck−Condon region becomes more extensive. As mentioned in the previous section, the geometric parameter that seems to influence the spectrum most sensitively is θ in eq 4, which measures the orientation of the OH bond of the excited H_2O, relative to an OH bond in a nearby, ground-state H_2O molecule. Figure 4 shows the distribution of θ values, where θ is the aforementioned torsion angle, for $(H_2O)_8$ at $T = 150$ K (solid line) and $T = 50$ K (dotted line). As expected, the range of θ values that are accessible at higher temperatures is considerably wider. The increased width with increasing T is partly due to the energy variation within excitonic states that are accessible both at low temperature and at high temperature and is partly due to the fact that some excitonic states are not accessible from low-temperature configurations, but become accessible for certain configurations at higher temperatures.

D. Multiple Peaks in the Electronic Absorption Spectrum. For small water clusters $(H_2O)_n$, for $n = 2-6$, initially in their

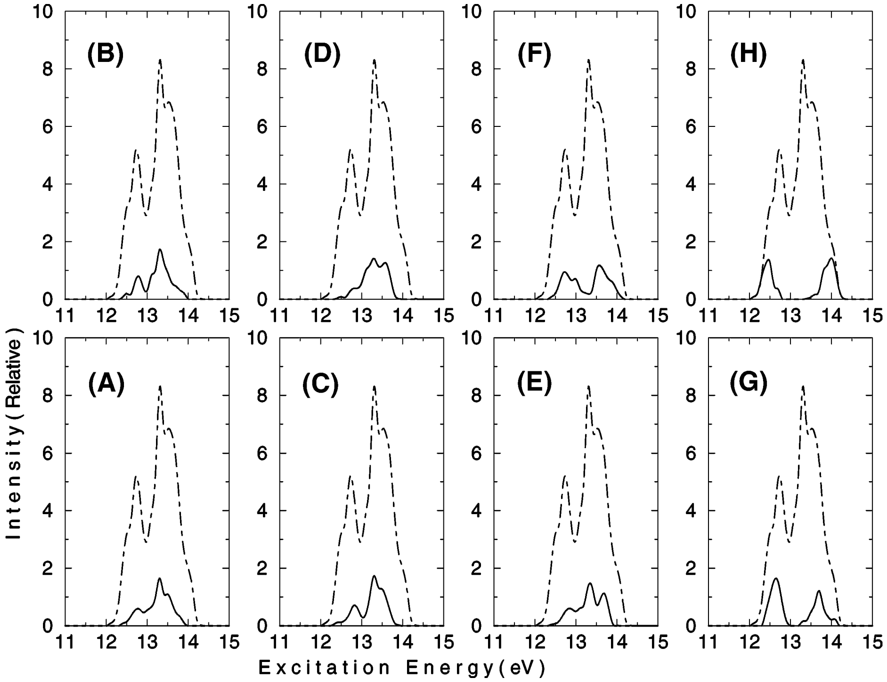

Figure 5. Contribution to the UV absorption intensity (dashed line) from the individual excitonic states (solid line), for $(H_2O)_8$ at $T = 50$ K: (A) first excitonic state, (B) second state, (C) third state, (D) fourth state, (E) fifth state, (F) sixth state, (G) seventh state, and (H) eighth state.

vibrational ground state, it seems that only a single, well-resolved absorption peak is found in the absorption spectrum.[32] However, Figure 3A shows three well-resolved peaks for $(H_2O)_8$ at $T = 50$ K. This multiple-peak structure disappears at $T = 300$ K. Three peaks are clearly observed in the total absorption band, and the more-detailed structure may not be realistic, given the limitations of the model. The multiple peaks are, in most cases, due to absorption into different excitonic states or groups of excitonic states. The splittings between different excitonic levels are so strong that the different peaks can survive even the broadening effects at quite high temperatures. The sensitivity of cluster spectra and, in particular, the occurrence of multiple peaks, depending on the temperature, is of considerable interest for future experimental studies.

E. Contributions of Different Excitonic States to the Spectrum. Figure 5 shows the absorption spectrum into each excitonic state of the cluster $(H_2O)_8$. In each of the cases, the full absorption intensity in the same region of excitation energies is also shown. As observed from the results, the spectral contribution of different excitonic states strongly overlap; however, the overlap is not complete. The results also show that, in most excitonic states, the absorption contributions of a single excitonic state exhibit a multiple-peak structure. The potential energy surface that is associated with each excitonic state varies strongly with energy, as a function of configuration. Excitation from different local minimum structures of the cluster may go into the same excitonic state; however, because of the different configurations, the energies will be quite different, resulting in possible different, well-resolved peaks. We note that the energetic order of the excitonic states is not necessarily the same for all configurations; i.e., potential surfaces that correspond to different electronic states have intersections in many cases.

F. Shift to the Red in the Low-Energy Tail. The absorption spectrum of the clusters are basically strongly shifted to the blue, with respect to the H_2O molecule. This basic feature leaves open the question whether an absorption tail to the red of the monomer can occur in the low-energy portion of the spectrum. Among the small $(H_2O)_n$ clusters ($n = 2-6$) initially in the vibrational ground state, only the dimer was also observed to possess an absorption tail to the red of the monomer.[32] This was attributed to the asymmetric structure of the dimer. Although the promoted electron in a cluster experiences mostly repulsive interactions, because of the O atoms of neighboring water molecules, in the case of the dimer, there is an additional attractive interaction mechanism. Consider the hydrogen-bond-donating molecule in the dimer. There is an attractive component to the interaction between the excited-state hydrogen-bond-donating water and the hydrogen-bond-accepting molecule. This is due to the high polarizability of the excited state, and inspection of the electronic wave function of the dimer shows that most of the electron density of the Rydberg-type orbital is polarized away from the negative charge on the neighboring O atom.[32] The attractive interaction reduces the excitation energy and results in the red tail of the dimer. The other clusters in the range of $n = 3-6$ have ring structures, the different molecules are almost symmetric, and the attractive mechanism does not occur. We researched whether such an effect of an absorption tail to the red of the monomer could be found for any of the larger clusters studied here, and the effect apparently is indeed unique to the dimer. On the other hand, there is an effect of an expanding absorption tail on the low-energy side of the spectrum with increasing temperature. Consider Figure 6, which compares the absorption spectra of $(H_2O)_8$ at $T = 250$ K and $T = 200$ K. The absorption tail at the lower energy is expanded to the red at the higher temperature. This effect is clearly due to the expansion of the Franck−Condon region as T increases, to include also configurations that give low excitation energies. These contributions seemingly result from configurations of lower symmetry, in which presumably the promoted electron experiences also attractive interactions with neighboring O atoms. However, the attraction is not sufficiently strong to produce a red shift, compared to the H_2O monomer.

IV. Concluding Remarks

In this paper, we presented a study of the electronic absorption spectroscopy of water clusters, based on a simple model of the

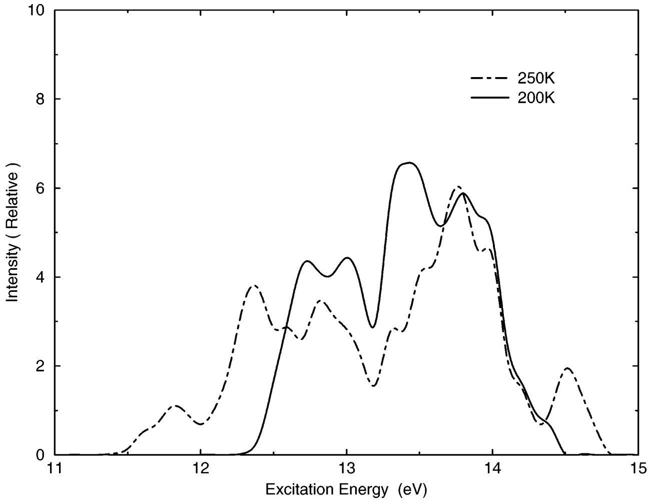

Figure 6. Electronic absorption spectrum of $(H_2O)_8$ (—) at $T = 200$ K and (− − −) at $T = 250$ K.

excited electronic states in the Franck−Condon region. The excitonic states were modeled in a framework that includes their dependence upon the intramolecular and intermolecular coordinates. This, together with classical molecular dynamics simulations of the initial states of the cluster, enabled us to calculate the UV absorption spectrum. The excitonic states and the dependence of their energies on nuclear configuration are the basis for interpreting the features of the spectra. Although the simplicity of the model and the lack of data concerning the excited states of water clusters means that the results are unlikely to be quantitatively accurate, they should provide useful qualitative insight.

Most of all, the intent of this study is to provide useful data for planning future experiments, and we believe such experiments to be feasible, given the present technology. However, precise selection of cluster size is not yet possible and experiments may need to be performed for a distribution of cluster sizes. Trends were observed, with regard to the dependence of the spectra on cluster size and temperature. These trends could be a useful target for experimental study. Other predictions, such as the occurrence of multiple, well-resolved absorption peaks for a given cluster, might also prove to be of experimental interest. We consider relative properties (e.g., relative spectral widths for different cluster sizes) to be the most useful for testing the model predictions against future experiments.

In the version presented here, the model used is very flexible and can readily be extended (to water in bulk, ice, water layers on surfaces, etc.). Adaptation of the model to other hydrogen-bonded clusters should also be straightforward.

Acknowledgment. This research was supported by the Israel Science Foundation (Grant No. 127/00-2, to R.B.G.). Work at the University of California at Irvine was supported by the National Science Foundation (NSF) (under CRC Grant No. CHE-0209719).

References and Notes

(1) Devlin, J. P., Buch, V., Eds.; *Water in Confined Geometries*; Springer: Berlin, 2003.

(2) Liu, K.; Cruzan, J. D.; Saykally, R. J. *Science* **1996**, *271*, 929.

(3) Nauta, K.; Miller, R. E. *Science* **2000**, *287*, 293.

(4) Buck, U.; Ettischer, I.; Melzer, M.; Buch, V.; Sadlej, J. *Phys. Rev. Lett.* **1998**, *80*, 2578.

(5) Gruenloh, C. J.; Carney, J. R.; Arrington, C. A.; Zwier, T. S.; Fredericks, S. Y.; Jordan, K. D. *Science* **1997**, *276*, 1678.

(6) Leforestier, C.; Braly, L. B.; Liu, K.; Elrod, M. J.; Saykally, R. J. *J. Chem. Phys.* **1997**, *106*, 8527.

(7) Devlin, J. P.; Joyce, C.; Buch, V. *J. Phys. Chem. A* **2000**, *104*, 1974.

(8) Sabo, D.; Bacic, Z.; Graf, S.; Leutwyler, S. *J. Chem. Phys.* **1998**, *109*, 5404.

(9) Losada, H.; Leutwyler, S. *J. Chem. Phys.* **2002**, *117*, 2003.

(10) Lee, H. H.; Kim, K. S. *J. Chem. Phys.* **2002**, *117*, 706.

(11) Keutsch, F. N.; Karyakin, N.; Saykally, R. J.; van der Avoird, A. *J. Chem. Phys.* **2001**, *114*, 3988.

(12) Xantheas, S. S.; Duning, T. H. *J. Chem. Phys.* **1993**, *99*, 8774.

(13) Chaban, G. M.; Jung, J. O.; Gerber, R. B. *J. Phys. Chem. A* **2000**, *104*, 2772.

(14) Gürtler, P.; Saile, V.; Koch, E. E. *Chem. Phys. Lett.* **1977**, *51*, 386.

(15) Klein, S.; Kochanski, E.; Strick, A.; Sadlej, A. *J. Theor. Chim. Acta* **1996**, *94*, 75.

(16) Dutuit, O.; Tabche-Fouhaile, A.; Nenner, I.; Frohlich, H.; Guyen, P. M. *J. Chem. Phys.* **1985**, *83*, 584.

(17) Andresen, P.; Ondrey, G. S.; Titze, B.; Rothe, E. W. *J. Chem. Phys.* **1984**, *80*, 2548.

(18) Lee, L. C.; Suto, M. *J. Chem. Phys.* **1986**, *110*, 161.

(19) Andresen, P.; Schinke, R. In *Molecular Photodissociation Dynamics*; Ashfold, M. N. R., Baggott, J. E., Eds.; Royal Society of Chemistry: London, 1987.

(20) Staemmler, V.; Palma, A. *Chem. Phys.* **1985**, *93*, 63.

(21) Theodorakopoulos, G.; Petsalakis, I. D.; Buenker, R. J. *J. Chem. Phys.* **1985**, *96*, 217.

(22) Schinke, R. *Photodissociation Dynamics*; Cambridge University Press: Cambridge, U.K., 1993.

(23) van Hemert, M.; van der Avoird, A. *J. Chem. Phys.* **1979**, *71*, 5310.

(24) Sosa, R. M.; Gardiol, P.; Ventura, O. N. *J. Mol. Struct.* **1993**, *297*, 337.

(25) Sobolewski, A. J.; Domcke, W., preprint, 2002.

(26) Thomsen, C. L.; Madsen, D.; Keiding, S. R.; Thogersen, J.; Christiansen, O. *J. Chem. Phys.* **1999**, *110*, 3453.

(27) Iwata, A.; Nakashima, N.; Izawa, Y.; Yamanaka, C. *Chem. Lett.* **1993**, *21*, 1939.

(28) McGowen, J. L.; Ajo, H. M.; Zhang, J. Z.; Schwatz, B. J. *Chem. Phys. Lett.* **1994**, *231*, 503.

(29) Bursulaya, B. D.; Jeon, J.; Yang, C.-N.; Kim, H. J. *J. Phys. Chem. A* **2000**, *104*, 45.

(30) Bursulaya, B. D.; Jeon, J.; Zichi, D. A.; Kim, H. J. *J. Chem. Phys.* **1998**, *108*, 3286.

(31) Christiansen, O.; Nymand, T. M.; Mikkelsen, K. V. *J. Chem. Phys.* **2000**, *113*, 8101.

(32) Harvey, J. N.; Jung, J. O.; Gerber, R. B. *J. Chem. Phys.* **1998**, *109*, 8747.

(33) Coker, D. F.; Watts, R. O. *J. Phys. Chem.* **1987**, *91*, 2513.

(34) Allen, M. P.; Tildesley, D. J. *Computer Simulations of Liquids*; Clarendon Press: Oxford, U.K., 1987.

(35) Engel, V.; Staemmler, V.; van der Waals, R. L.; Crim, F. F.; Sension, R. J.; Hudson, B.; Andresen, P.; Henning, S.; Weide, K.; Schinke, R. *J. Phys. Chem.* **1992**, *96*, 3201.

(36) Balkova, A.; Bartlett, R. J. *J. Chem. Phys.* **1993**, *99*, 7907.

(37) Stone, A. J. *The Theory of Intermolecular Forces*; Clarendon Press: Oxford, U.K., 1996.

(38) Engel, V.; Schinke, R.; Staemmler, V. *J. Chem. Phys.* **1988**, *88*, 129.

(39) Imura, K.; Veneziani, M.; Kasai, T. In *Advances in Atomic and Molecular Beams*; Springer−Verlag: Berlin, 2000.